Projection of the Danzer tiling

1994 J. Phys. A: Math. Gen. 27 4505

(http://iopscience.iop.org/0305-4470/27/13/024)

J. Phys. A: Math. Gen. 27 (1994) 4505–4517. Printed in the UK

Projection of the Danzer tiling

P Kramer, Z Papadopolos, M Schlottmann and D Zeidler
Institut für Theoretische Physik der Universität, D-72076 Tübingen, Germany

Received 9 December 1993, in final form 28 April 1994

Abstract. We derive the icosahedrally-symmetric octahedral tiling of Danzer, denoted by $\mathcal{T}^{(D)}$, locally from the tiling $\mathcal{T}^{(2F)}$ of Kramer *et al*, obtained by icosahedral projection from the root lattice D_6. Moreover, we determine all windows such that the tiling $\mathcal{T}^{(D)}$ can be obtained by projection from the 6D root lattice D_6. We reconstruct all vertex configurations of the tiling $\mathcal{T}^{(D)}$ using the tools of the projection method.

1. Introduction

The icosahedrally-symmetric Danzer octahedral tiling that we will denote by $\mathcal{T}^{(D)}$ was obtained by Danzer by inflation [1,2]. The four tiles of the tiling $\mathcal{T}^{(D)}$ are presented in figure 1 (see also [2]). The tiling $\mathcal{T}^{(D)}$ is locally equivalent [3] to Danzer tetrahedral tiling [2]: dissecting Danzer's octahedra (figure 1) by all their mirror symmetry planes, one obtains Danzer's tetrahedra, whereas in every tetrahedral tiling the tetrahedra can be glued together to form octahedra in a locally unique fashion.

From diffraction experiments, a class of icosahedral quasicrystals has been described [4] in terms of the $\mathbb{Z}$ module projected from the face-centred hypercubic F-lattice in six dimensions, the root lattice D_6 [5]. Models for the atomic positions and diffraction properties of these quasicristals are facilitated by the construction of tilings projected from this lattice.

The icosahedrally-symmetric tiling $\mathcal{T}^{(2F)}$ has been obtained by projection from the six-dimensional (6D) root lattice D_6 [6]. The scale of lengths is defined by the D_6 basis vectors $e_2 - e_1$, $e_3 - e_2$, $e_4 - e_3$, $e_5 - e_4$, $e_6 - e_5$, $-e_5 - e_6$ expressed by the 6D standard base e_i, $(e_i, e_j) = \delta_{ij}$, $i, j = 1, 2 \ldots 6$. Associated with the root lattice D_6 there are two mutually dual cell complexes, the Voronoi complex $\mathcal{V}$ and the Delaunay complex $\mathcal{V}^*$, each with a full hierarchy of m-dimensional boundaries (m-boundaries) P and dual (6-m)-dimensional boundaries P^*, respectively ($m \leqslant 6$). The dual boundary P^* of the boundary P of the Voronoi domain is defined as the convex hull of all lattice points whose Voronoi domains contain the boundary P. The boundaries obey the duality relation [7,8]

$$P_1^* \subseteq P_2^* \Leftrightarrow P_1 \supseteq P_2. \tag{1}$$

Under the action of the icosahedral group, the 6D space decomposes into two irreducible orthogonal subspaces $\mathbb{E}_\parallel$ and $\mathbb{E}_\perp$. In what follows, the tiling $\mathcal{T}^{(2F)}$ will be built from the parallel projections of 3-boundaries $P \in \mathcal{V}$, the tiles. The tiles, their faces, edges and vertices will be coded by so-called windows [3] which are perpendicular projections of dual boundaries $P^* \in \mathcal{V}^*$, dual to the preimages of the tiles, their faces edges and vertices in 6D, respectivly. For the coding, the relation for 3-boundaries $P_1, P_2 \in \mathcal{V}$

$$P_{1\perp}^* \cap P_{2\perp}^* \neq \phi \Rightarrow P_{1\parallel} \cap P_{2\parallel} = [P_1 \cap P_2]_\parallel \tag{2}$$

0305-4470/94/134505+13\$19.50

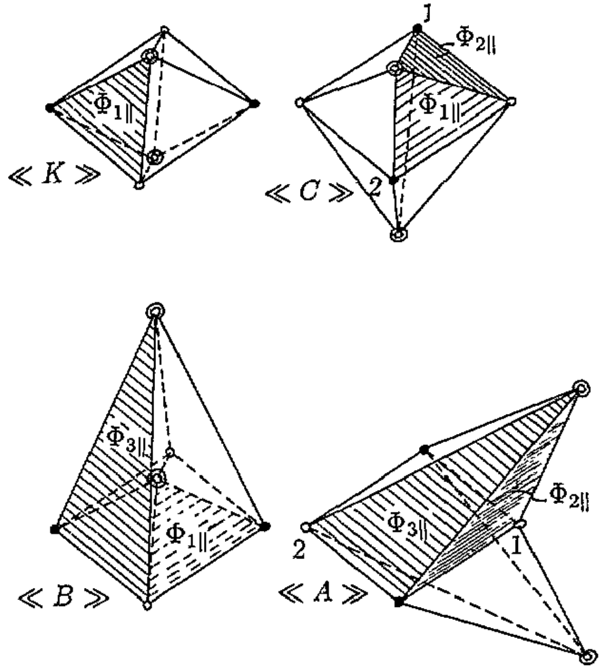

Figure 1. Danzer's octahedra $\langle\langle X \rangle\rangle$ where $X = K, C, B, A$. $\langle\langle B \rangle\rangle$ and $\langle\langle A \rangle\rangle$ are not convex. The three different types of vertices a, b and c are denoted by black, double white and single white circles, respectively (Danzer denoted them 2, 1 and 3, respectively). The numbers 1 and 2 on the figure denote two different vertices of the same type on the same octahedra but with different space angle. For 2D faces denoted by $\Phi_{i\|}$, $i = 1, 2, 3$ see figure 2.

following from the results of [8] is essential. The subscript $\|$ denotes the projection onto $\mathbb{E}_\|$, $\perp$ onto $\mathbb{E}_\perp$.

The vertex set of $\mathcal{T}^{(2F)}$ is obtained [6] by the parallel projection of certain holes of the lattice D_6. The holes [5] are the vertices of its Voronoi domains. The choice of the holes to be projected onto $\mathbb{E}_\|$ is made with the help of atomic surfaces, or vertex windows, in the form of icosahedrally projected Delaunay cells into $\mathbb{E}_\perp$. The canonical choice of the representative Delaunay cells forming a fundamental domain of the root lattice is determined by the fundamental simplex [5]. It turns out that in the case D_6 one has three canonical Delaunay cells, denoted by D^a, D^b and D^c, as dual objects to the canonical holes at $a = \frac{1}{2}(111111)$, $b = (100000)$ and $c = \frac{1}{2}(11111\bar{1})$, respectively [6]. Any other Delaunay cell $D^{x'}$ of type a, b or c, respectively, in the lattice D_6, may be written as

$$D^{x'} = D^{x+t} = D^x + t, \qquad t \in D_6, \tag{3}$$

where $x = a, b$ or c, respectively. The canonical Delaunay cells intersect in 5-boundaries: $D^a \cap D^b = \beta_1^*$, $D^a \cap D^c = \alpha^*$ and $D^b \cap D^c = \gamma_2^*$ (for the notation see [6]).

The procedure for constructing the tiling $\mathcal{T}^{(2F)}$ is:

(0) Choose a 'shift vector' $s_\perp \in \mathbb{E}_\perp$, suppose $s_\perp \in D^a_\perp$.

(1) Find all dual 3-subboundaries $P^{\mu *}$ of D^a such that $s_\perp \in P^{\mu *}_\perp$.

(2) Construct in $\mathbb{E}_\|$ the vertex configuration $v^a_\|$

$$v^a_\| = \bigcup_\mu P^{\mu *}_\| . \tag{4}$$

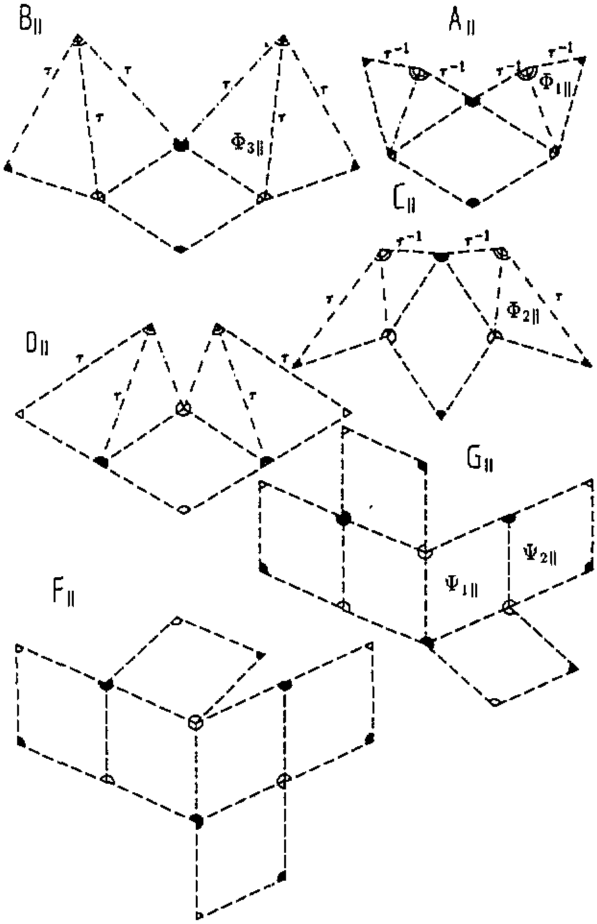

Figure 2. The tiles of the tiling $\mathcal{T}^{(2F)}$. Edges run along five-fold (– – –) or three-fold (— · —) axes. Scalings by powers of τ with respect to the standard length are marked for each type of axis. Vertices of type a, b, c are denoted as in figure 1. $\Phi_{i\|}$, $i = 1, 2, 3$ and $\Psi_{1\|}$ and $\Psi_{2\|}$ are 2D faces.

(3) Run along each edge starting at the centre $a_{\|}$ of the vertex configuration $v_{\|}^{a}$. Lift† the next vertex $x'_{\|}$ into 6D to a hole x'. It is going to be of a different type, say, of type b. Determine $t = x' - b \in D_6$.

(4) Let $s'_{\perp} = s_{\perp} - t_{\perp}$; then $s'_{\perp} \in D_{\perp}^{b}$ return to (1) replacing $s_{\perp}$ by $s'_{\perp}$ and a by b.

The tiles in the tiling $\mathcal{T}^{(2F)}$ are [6] four pyramids, acute and obtuse rhombohedra, presented in figure 2 by unfolding the polytopes into a plane. To describe the edges of the projected polytopes, we introduce the symbols: ② denotes an edge of length $(2/(\tau+2))^{1/2}$ running along any two-fold axes, ③ an edge of length $(3/(2(\tau+2)))^{1/2}$ along three-fold axes and ⑤ an edge of length $1/\sqrt{2}$ along five-fold axes‡. Powers of τ in front of these standard edges denote corresponding scalings. The faces of the tiles are either rhombus-shaped with edges ⑤ and short diagonal ② or triangular-shaped with edges scaled from ③

† The lifting of the vertices of the tiling $\mathcal{T}^{(2F)}$ from 3D space $\mathbb{E}_{\|}$ into D_6-holes is unique.

‡ $\tau = (1+\sqrt{5})/2$.

and ⑤. All faces of triangular shape, $\Phi_{1\|}$, $\Phi_{2\|}$, $\Phi_{3\|}$ (figures 1 and 2), and only these, also appear in the Danzer tiling.

For our investigation, the rhombus-shaped faces in $\mathcal{T}^{(2F)}$ which do not appear in $\mathcal{T}^{(D)}$ are of particular interest. *In the* D_6 *Voronoi complex there are triangular and square two-*boundaries denoted by Φ and Ψ, respectively. Under the action of the group $D_6 \times_s I_h$ there are two non-equivalent two-boundaries Ψ_1 and Ψ_2. They are such that when projected to $\mathbb{E}_\|$, Ψ_1 and Ψ_2 appear as two congruent rhombi but with a different distribution of vertices of type a and c, see figure 3. One can show that any rhombus face in the tiling $\mathcal{T}^{(2F)}$ can be identified as $\Psi_{1\|}$ or $\Psi_{2\|}$ from its local surrounding, i.e. the 'decoration' of rhombus faces by the appropriate vertices can be locally derived: (1) Any pyramid† has a uniquely fixed basis: $C_\|$ and $D_\|$ have a basis of type $\Psi_{1\|}$, $A_\|$ and $B_\|$ of type $\Psi_{2\|}$. (2) Any $F_\|$ appears in the tiling with three $D_\|$ pyramids [9], $F_\| \cup 3D_\|$ (figure 4(*a*)). The tile $F_\|$ shares with every $D_\|$ the face $\Psi_{1\|}$. (3) Any $G_\|$ has at least one rhombus face in common with a pyramid which identifies all its vertices.

In what follows we derive the tiling $\mathcal{T}^{(D)}$ from the tiling $\mathcal{T}^{(2F)}$ and give in detail its projection from the root lattice D_6. By the unique lifting of the vertices of $\mathcal{T}^{(D)}$ into the D_6-holes, we determine the vertex windows for the three types of Danzer vertices denoted by 1, 2 and 3. We identify the Danzer vertices: 2, 1 and 3 with the representative holes of the D_6-lattice $a = \frac{1}{2}(111111)$, $b = (100000)$ and $c = \frac{1}{2}(11111\bar{1})$, respectively, as anticipated in figure 1. The vertex windows for $\mathcal{T}^{(D)}$ have been previously numerically derived by van Ophuysen [10]. We determine all the vertex configurations for $\mathcal{T}^{(D)}$ by the projection-window method.

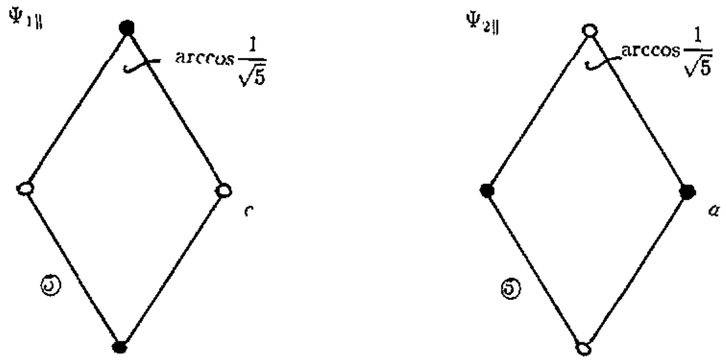

Figure 3. Rhombus faces $\Psi_{1\|}$ and $\Psi_{2\|}$. Edges run along five-fold axes of standard length ⑤$= |e_{j\|}|$, $j = 1, 2, \ldots, 6$.

2. Derivation of the tiling $\mathcal{T}^{(D)}$ from the tiling $\mathcal{T}^{(2F)}$

We present the results of the local derivation of the tiling $\mathcal{T}^{(D)}$ from the tiling $\mathcal{T}^{(2F)}$ and produce all the windows needed for the projection of $\mathcal{T}^{(D)}$. In the proofs of the derivation and determination of the windows, one proceeds in $\mathbb{E}_\|$ and $\mathbb{E}_\perp$ simultaneously, eliminating in $\mathbb{E}_\|$ the rhombus faces $\Psi_{1\|}$ and $\Psi_{2\|}$. In order to decide which pairs of tiles in $\mathbb{E}_\|$ (in the

† Notice that the top of each pyramid $A_\|$, $B_\|$, $C_\|$ or $D_\|$ is of type b.

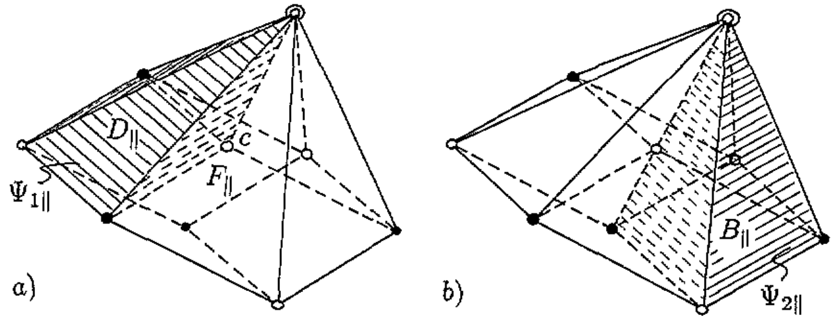

Figure 4. (*a*) The $F_\| \cup 3D_\|$ configuration; (*b*) the $3B_\|$ configuration.

case of $\mathcal{T}^{(2F)}$, two three-boundaries of Voronoi cell projected into $\mathbb{E}_\|$) can appear in the tiling with a common two-boundary $\Psi_{i\|}$ $i = 1, 2$, we have to study the corresponding dual four-boundary $\Psi^*_{i\perp}$ and the full content of its three-subboundaries. The three-subboundaries of $\Psi^*_{i\perp}$ that have non-trivial mutual intersection in $\mathbb{E}_\perp$ give rise to the appearance of their dual three-boundaries in the tiling $\mathcal{T}^{(2F)}$ with a common $\Psi_{i\|}$. This criterion is the consequence of relations (1) and (2).

2.1. *Local derivation of Danzer's tiling from the tiling $\mathcal{T}^{(2F)}$*

The local derivation of $\mathcal{T}^{(D)}$ from $\mathcal{T}^{(2F)}$ can be performed in five steps which we describe in the following using some simple observations on the tiling $\mathcal{T}^{(2F)}$ without proving them in detail.

(1) The obtuse rhombohedron $F_\|$ always appears in $\mathcal{T}^{(2F)}$ with three $D_\|$ pyramids, each sharing with $F_\|$ one of its faces $\Psi_{1\|}$, (cf figure 4(*a*)). This is simultaneously a vertex configuration of type c (c.1, see [9]). The configuration $F_\| \cup 3D_\|$ is to be transformed into a $3B_\|$ configuration (according to figure 4(*b*)):

$$F_\| \cup 3D_\| \longrightarrow 3B_\|. \tag{5}$$

By this transformation, the vertex configuration c.1 disappears, therefore the window for the vertex configuration which is the window $F^*_\perp$ has to be subtracted from the vertex window $D^c_\perp$. The result turns out to be as shown in figure 11.

(2) The remaining $D_\|$ pyramids with no $\Psi_{1\|}$ faces in common with some obtuse rhombohedron all appear in pairs sharing $\Psi_{1\|}$ such that they are mirror images of each other with respect to the plane containing $\Psi_{1\|}$. These pairs are transformed into Danzer's octahedra $\langle\langle A\rangle\rangle$:

$$2D_\| \longrightarrow \langle\langle A\rangle\rangle. \tag{6}$$

(3) The acute rhombohedron $G_\|$ can be subdivided into a new vertex configuration of type b:

$$G_\| \longrightarrow 3A_\| \cup 3C_\| \tag{7}$$

see figure 5. The window for the new vertex configuration of type b, that is the window $G^*_\perp$, has to enlarge the vertex window $D^b_\perp$, see section 2.3.

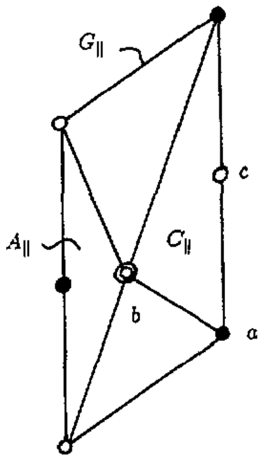

Figure 5. The acute rhombohedron $G_\parallel$ transformed into the configuration $3A_\parallel \cup 3C_\parallel$.

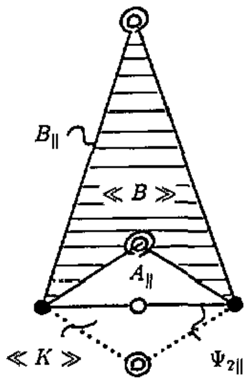

Figure 6. The pyramid $B_\parallel$ transformed into Danzer's octahedron $\langle\langle B\rangle\rangle$ and the pyramid $A_\parallel$.

(4) All pyramids of type $B_\parallel$, originally existing in the tiling $\mathbb{E}_\parallel$, and those obtained after step (1), are *transformed into Danzer's octahedra* $\langle\langle B\rangle\rangle$ *and the pyramid of the shape* $A_\parallel$:

$$B_\parallel \longrightarrow \langle\langle B\rangle\rangle \cup A_\parallel \tag{8}$$

see figure 6. The new vertex of type b, (i) stemming from the transformation of the originally existing $B_\parallel$ in $\mathbb{E}_\parallel$, has the window $B^*_\perp$; and (ii) stemming from the transformation of the tiles $B_\parallel$ obtained after step (1) has the window $F^*_\perp$. See section 2.3.

(5a) As a consequence of the previous steps, all pyramids $A_\parallel$ originally existing in $\mathbb{E}_\parallel$ and those obtained after steps (3) and (4) appear in pairs with the common face $\Psi_{2\parallel}$. These pairs are transformed into Danzer's octahedra $\langle\langle K\rangle\rangle$:

$$2A_\parallel \longrightarrow \langle\langle K\rangle\rangle. \tag{9}$$

(5b) All pyramids $C_\parallel$, originally existing in $\mathbb{E}_\parallel$ and those obtained after step (3), appear in pairs with the common face $\Psi_{1\parallel}$. They are mutually mirror images with respect to the

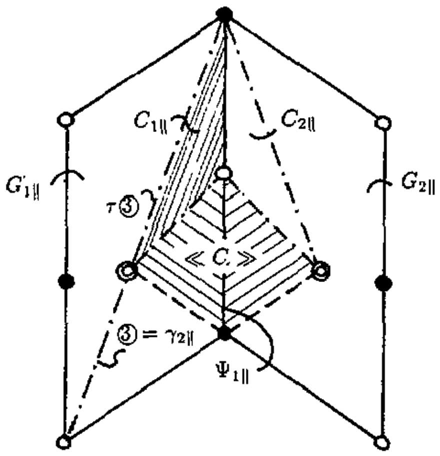

Figure 7. Transformations in $\mathcal{T}^{(2F)}$ leading to Danzer's octahedron $\langle\langle C\rangle\rangle$.

plane containing the common $\Psi_{1\|}$. These pairs are transformed into Danzer's octahedra $\langle\langle C\rangle\rangle$ as in figure 7:

$$2C_{\|} \longrightarrow \langle\langle C\rangle\rangle. \tag{10}$$

After these transformations, a tiling is obtained which consists of Danzer's octahedra in a face-to-face arrangement, i.e. Danzer's tiling.

The inverse procedure, a local derivation of the tiling $\mathcal{T}^{(2F)}$ from the tiling $\mathcal{T}^{(D)}$, is not possible: an inspection of the windows of $\mathcal{T}^{(D)}$ tiles (see section 2.2) shows that each face is orthogonal to a five-fold axis with respect to the icosahedral group acting in $\mathbb{E}_{\perp}$. On the other hand, the $\mathcal{T}^{(2F)}$-windows are bounded by faces orthogonal to five-fold and three-fold axes. Hence, it is not possible to construct all $\mathcal{T}^{(2F)}$-windows by finite unions and intersections of $\mathcal{T}^{(D)}$-windows. This implies the impossibility of a local derivation [3] of the tiling $\mathcal{T}^{(2F)}$ from the tiling $\mathcal{T}^{(D)}$.

2.2. *The windows for the tiles of* $\mathcal{T}^{(D)}$

One determines the windows of Danzer's octahedra from those of $\mathcal{T}^{(2F)}$ [6, 11] following the transformation procedure outlined in section 2.1.

(1) The octahedron $\langle\langle C\rangle\rangle$ is obtained wherever a rhombus $\Psi_{1\|}$ occurs with a $G_{\|}$ or $C_{\|}$ tile in $\mathcal{T}^{(2F)}$. Therefore,

$$\langle\langle C\rangle\rangle^{w} = C_{\perp}^{*} \cup G_{\perp}^{*}. \tag{11}$$

(2) The octahedron $\langle\langle A\rangle\rangle$ is due to the pairs of pyramids $D_{\|}$ in $\mathcal{T}^{(2F)}$ sharing a face $\Psi_{1\|}$:

$$\langle\langle A\rangle\rangle^{w} = D_{1\perp}^{*} \cap D_{2\perp}^{*}. \tag{12}$$

(3) The octahedron $\langle\langle B\rangle\rangle$ is induced either by the pyramid $B_{\|}$ or by the obtuse rhombohedron $F_{\|}$; there are two possible $F_{\|}$ for a certain $\langle\langle B\rangle\rangle$:

$$\langle\langle B\rangle\rangle^{w} = F_{1\perp}^{*} \cup B_{\perp}^{*} \cup F_{2\perp}^{*}. \tag{13}$$

(4) The octahedron $\langle\langle K\rangle\rangle$ is positioned just at the rhombi $\Psi_{2\|}$ in $\mathcal{T}^{(2F)}$:

$$\langle\langle K\rangle\rangle^{w} = \Psi_{2\perp}^{*} = G_{1\perp}^{*} \cup G_{2\perp}^{*} \cup B_{\perp}^{*} \cup A_{\perp}^{*} \cup F_{1\perp}^{*} \cup F_{2\perp}^{*}. \tag{14}$$

For the notation see figures 8, 9 and 10. They depict the $\mathcal{T}^{(D)}$-windows embedded in the four-boundaries $\Psi_{1\perp}^{*}$ and $\Psi_{2\perp}^{*}$.

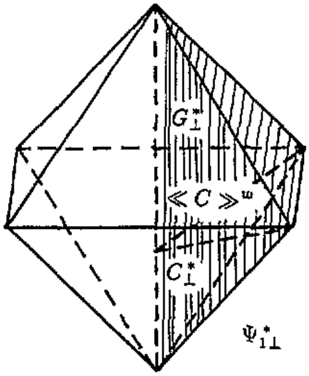

Figure 8. The window $\langle\langle C\rangle\rangle^w$ in $\mathbb{E}_\perp$ for Danzer's octahedron $\langle\langle C\rangle\rangle$ in $\mathbb{E}_\parallel$.

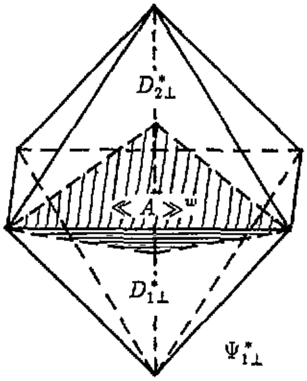

Figure 9. The window $\langle\langle A\rangle\rangle^w$ in $\mathbb{E}_\perp$ for Danzer's octahedron $\langle\langle A\rangle\rangle$ in $\mathbb{E}_\parallel$.

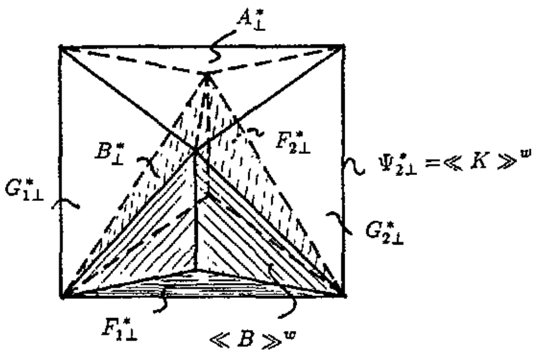

Figure 10. The window $\langle\langle B\rangle\rangle^w$ for Danzer's octahedron $\langle\langle B\rangle\rangle$ and the window $\langle\langle K\rangle\rangle^w$ for Danzer's octahedron $\langle\langle K\rangle\rangle$.

2.3. The vertex windows for the tiling of $\mathcal{T}^{(D)}$, windows for tiles of $\mathcal{T}^{(D)}$ and their orbit representatives with respect to $D_6 \times {}_s\mathrm{I}_h$ reduced to the vertex windows of $\mathcal{T}^{(D)}$

The vertex windows for the tiling $\mathcal{T}^{(D)}$ are labelled by $\tilde{D}^a_\perp$, $\tilde{D}^c_\perp$ and $\tilde{D}^b_\perp$.

The vertex window for the vertices of type a is the same as for $\mathcal{T}^{(2F)}$, $\tilde{D}^a_\perp = D^a_\perp$. It is a dodecahedron with the edge of length ②

The vertex window for the vertices of type c is presented in figure 11. Its form is the consequence of step (1) in the local derivation in section 2.1.

Table 1. Volumes of $D^a_\perp, D^b_\perp, D^c_\perp$ and $\tilde{D}^a_\perp, \tilde{D}^b_\perp, \tilde{D}^c_\perp$ given in units of V.

x	$D^{(x)}_\perp$	$\tilde{D}^{(x)}_\perp$
a	$6(7\tau+4)$	$6(7\tau+4)$
b	$10(\tau+1)$	$30(5\tau+2)$
c	$10(5\tau+3)$	$30(\tau+1)$

The vertex window for the vertices of type b, $\tilde{D}^b_\perp$ is presented in figure 12. Its form is obtained after adding the windows for the additional vertex configurations at appropriate

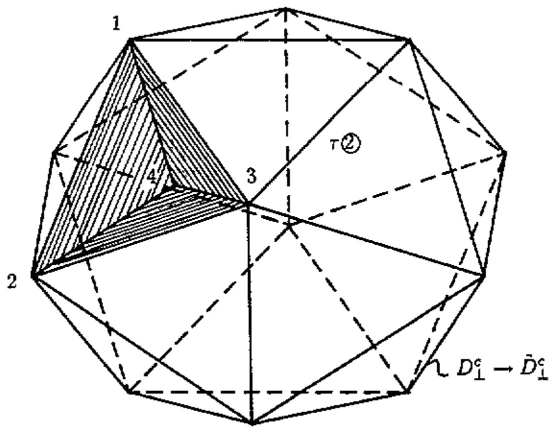

Figure 11. The vertex window $\tilde{D}^c_\perp$. Subtracted representative window $F^*_\perp = \langle 1,2,3,4\rangle \equiv \langle \frac{1}{2}(11\bar{1}\bar{1}1\bar{1}), \frac{1}{2}(\bar{1}11\bar{1}1\bar{1}), \frac{1}{2}(1\bar{1}1\bar{1}1\bar{1}), \frac{1}{2}(\bar{1}\bar{1}\bar{1}\bar{1}1\bar{1})\rangle_\perp$ for the vertex configuration $c.1$ [9] is denoted. The origin of the coordinate system is in the centre of the polytope $D^c_\perp$.

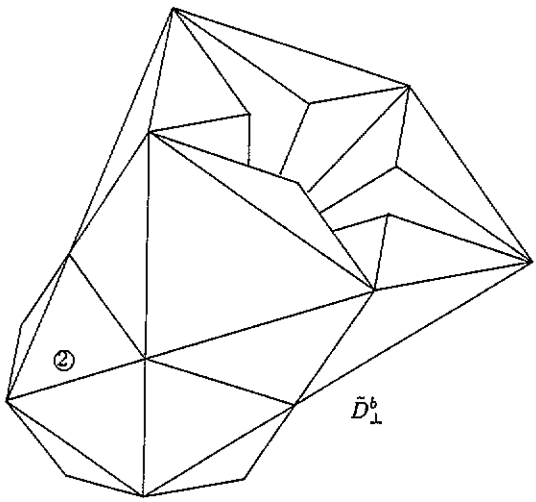

Figure 12. The vertex window $\tilde{D}^b_\perp$ is a dodecahedral extension of the icosahedral Delaunay cell $D^b_\perp$. A representative part of this extension is shown.

places. The additional vertex configurations of type b appear after the transformation steps (3) and (4) in section 2.1.

The volumes of the vertex windows of the tilings $\mathcal{T}^{(\mathrm{D})}$ and $\mathcal{T}^{(2\mathrm{F})}$ are given in table 1 in units of $V = \frac{2}{3}(1/(5+\sqrt{5})^3)^{1/2}$.

The positions of the windows for Danzer's octahedra in $\tilde{D}^a_\perp$ and $\tilde{D}^c_\perp$ can be easily determined from the positions of the four-boundaries $\Psi^*_{1\perp}$ and $\Psi^*_{2\perp}$ in $D^a_\perp$ and $D^c_\perp$. Their positions within $\Psi^*_{1\perp}$ and $\Psi^*_{2\perp}$ are given in figures 8, 9 and 10 in section 2.2. In this section we also expressed the windows $\langle\langle C\rangle\rangle^w$, $\langle\langle A\rangle\rangle^w$, $\langle\langle B\rangle\rangle^w$ and $\langle\langle K\rangle\rangle^w$ through three-boundaries $F^*_\perp$, $G^*_\perp$, $A^*_\perp$, $B^*_\perp$, $C^*_\perp$ and $D^*_\perp$, the windows for tiles of the tiling $\mathcal{T}^{(2\mathrm{F})}$, by the relations (11), (12), (13) and (14), respectively. We use these relations in order to determine

Table 2. Orbit representatives of windows $\langle\langle X\rangle\rangle^w$ with respect to the action of the groups $\mathrm{I_h}$ and $\mathrm{D_6} \times_s \mathrm{I_h}$ reduced to the vertex window $\tilde{D}^a_\perp$ and corresponding Danzer's octahedra $\langle\langle X\rangle\rangle$. The centre of $\tilde{D}^a_\perp$ is $a = \frac{1}{2}(111111)$ icosahedrally projected to $\mathbb{E}_\perp$. Notation: (i) the symbol $\langle\ldots\rangle$ means the simplex with given vertices; (ii) $P(111100) \circ e_1 \equiv \mu[\frac{1}{2}(e_1 + e_2 + e_3 + e_4) + \frac{1}{2}\sum_{i=5,6} \lambda_i e_i] + (1-\mu)e_1$ where $\mu \epsilon [0, 1], \lambda_i \epsilon [-1, 1]$.

X	$\langle\langle X\rangle\rangle^w$	$\langle\langle X\rangle\rangle$	$\mathrm{I_h}$ o.l.	$\mathrm{D_6} \times_s \mathrm{I_h}$ o.l.
$C(1)$	$\langle e_1+e_2, e_1+e_3, e_1+e_4, e_2+e_4\rangle_\perp$	$[P(111100)\circ e_1]_\parallel \cup$ $[P(111100)\circ(e_1+e_2+e_4)]_\parallel$	30	60
$C(2)$	$\langle e_1+e_3, e_2+e_3, e_3+e_4, e_2+e_4\rangle_\perp$	$[P(111100)\circ e_3]_\parallel \cup$ $[P(111100)\circ(e_2+e_3+e_4)]_\parallel$	30	
A	$\langle 0, e_1+e_4, e_3+e_4,$ $e_1+e_2+e_3+e_4\rangle_\perp$	$[P(111100)\circ e_4]_\parallel \cup$ $[P(111100)\circ(e_1+e_3+e_4)]_\parallel$	60	60
B	$[\langle 0, e_1-e_4, e_3-e_4, e_1+e_3\rangle_\perp \cup$ $\langle 0, e_1-e_4, e_3-e_4, e_2-e_4\rangle_\perp \cup$ $\langle e_1-e_4, e_3-e_4, e_2-e_4,$ $e_1+e_2+e_3-e_4\rangle_\perp]$ $+(e_4+e_6)_\perp$	$\{[P(111\bar{1}00)\circ(-e_4)]_\parallel \backslash$ $[P(111\bar{1}00)\circ e_2]_\parallel\}$ $+(e_4+e_6)_\parallel$	60	60
K	$\langle\langle B\rangle\rangle^w \cup$ $\{[\langle e_2+e_3, e_1+e_2, 0, e_2-e_4\rangle_\perp \cup$ $\langle e_2+e_3, 0, e_2-e_4, e_3-e_4\rangle_\perp \cup$ $\langle 0, e_2-e_4, e_1+e_2, e_1-e_4\rangle_\perp]$ $+(e_4+e_6)_\perp\}$	$\{[P(111\bar{1}00)\circ e_2]_\parallel \cup$ $[P(111\bar{1}00)\circ(e_1+e_3-e_4)]_\parallel\}$ $+(e_4+e_6)_\parallel$	30	30

Table 3. Orbit representatives of windows $\langle\langle X\rangle\rangle^w$ with respect to the action of the groups $\mathrm{I_h}$ and $\mathrm{D_6} \times_s \mathrm{I_h}$ reduced to the vertex window $\tilde{D}^b_\perp$ and corresponding Danzer's octahedra $\langle\langle X\rangle\rangle$. The centre of $\tilde{D}^b_\perp$ is $b = (100000)$ icosahedrally projected to $\mathbb{E}_\perp$. Notations as in table 2.

X	$\langle\langle X\rangle\rangle^w$	$\langle\langle X\rangle\rangle$	$\mathrm{I_h}$ o.l.	$\mathrm{D_6} \times_s \mathrm{I_h}$ o.l.
C	$\langle e_1+e_2, e_1+e_3, e_1+e_4, e_2+e_4\rangle_\perp$	$[P(111100)\circ e_1]_\parallel \cup$ $[P(111100)\circ(e_1+e_2+e_4)]_\parallel$	60	60
A	$\langle 0, e_1+e_2, e_1-e_3, -e_3-e_4\rangle_\perp$	$[P(11\bar{1}\bar{1}00)\circ e_1]_\parallel \cup$ $[P(11\bar{1}\bar{1}00)\circ(-e_3)]_\parallel$	60	60
$B(1)$	$[\langle -e_2+e_3, e_1-e_2, 0, e_1+e_3\rangle_\perp \cup$ $\langle -e_2+e_3, e_1-e_2, 0, -e_2+e_4\rangle_\perp \cup$ $\langle -e_2+e_3, e_1-e_2, -e_2+e_4,$ $e_1-e_2+e_3+e_4\rangle_\perp]$ $+(e_1-e_4)_\perp$	$\{[P(1\bar{1}1100)\circ(-e_2)]_\parallel \backslash$ $[P(1\bar{1}1100)\circ e_4]_\parallel\}$ $+(e_1-e_4)_\parallel$	30	60
$B(2)$	$\langle 0, e_1-e_3, e_1-e_4, -e_3-e_4\rangle_\perp \cup$ $\langle 0, e_1-e_3, e_1-e_4, e_1-e_2\rangle_\perp \cup$ $\langle 0, e_1-e_3, e_1-e_2, -e_2-e_3\rangle_\perp$	$[P(1\bar{1}\bar{1}\bar{1}00)\circ e_1]_\parallel \backslash$ $[P(1\bar{1}\bar{1}\bar{1}00)\circ(e_1-e_2-e_4)]_\parallel$	30	
K	$\langle\langle B(1)\rangle\rangle^w \cup$ $\{[\langle 0, -e_2+e_4, -e_2+e_3, e_3+e_4\rangle_\perp \cup$ $\langle 0, -e_2+e_4, e_1+e_4, e_1-e_2\rangle_\perp \cup$ $\langle 0, -e_2+e_4, e_1+e_4, e_3+e_4\rangle_\perp]$ $+(e_1-e_4)_\perp\}$	$\{[P(1\bar{1}1100)\circ e_4]_\parallel \cup$ $[P(1\bar{1}1100)\circ(e_1-e_2+e_3)]_\parallel\}$ $+(e_1-e_4)_\parallel$	30	30

the positions of the windows of Danzer's octahedra in the vertex window $\tilde{D}^b_\perp$. The results are presented in tables 2–4

Table 4. Orbit representatives of windows $\langle\langle X\rangle\rangle^w$ with respect to the action of the groups I_h and $D_6 \times_s I_h$ reduced to the vertex window $\tilde{D}_\perp^c$ and corresponding Danzer's octahedra $\langle\langle X\rangle\rangle$. The centre of $\tilde{D}_\perp^c$ is $c = \frac{1}{2}(11111\bar{1})$ icosahedrally projected to $\mathbb{E}_\perp$. Notations as in (a).

X	$\langle\langle X\rangle\rangle^w$	$\langle\langle X\rangle\rangle$	I_h o.l.	$D_6 \times_s I_h$ o.l.
C	$\langle e_1+e_3, e_2+e_3, e_3+e_4, e_2+e_4\rangle_\perp$	$[P(111100)\circ e_3]_\parallel \cup$ $[P(111100)\circ(e_2+e_3+e_4)]_\parallel$	60	60
$A(1)$	$\langle 0, e_1+e_4, e_3+e_4,$ $e_1+e_2+e_3+e_4\rangle_\perp$	$[P(111100)\circ e_4]_\parallel \cup$ $[P(111100)\circ(e_1+e_3+e_4)]_\parallel$	30	60
$A(2)$	$\langle 0, e_1+e_2, e_2+e_3,$ $e_1+e_2+e_3+e_4\rangle_\perp$	$[P(111100)\circ e_2]_\parallel \cup$ $[P(111100)\circ(e_1+e_2+e_3)]_\parallel$	30	
B	$[\langle e_2-e_1, e_2+e_3, e_2+e_4,$ $-e_1+e_2+e_3+e_4\rangle_\perp \cup$ $\langle e_2+e_3, e_2+e_4, e_3+e_4,$ $-e_1+e_2+e_3+e_4\rangle_\perp \cup$ $\langle e_2+e_4, e_3+e_4, -e_1+e_4,$ $-e_1+e_2+e_3+e_4\rangle_\perp]$ $+(e_1-e_6)_\perp$	$\{[P(\bar{1}11100)\circ(e_2+e_3+e_4)]_\parallel \setminus$ $[P(\bar{1}11100)\circ e_3]_\parallel\}$ $+(e_1-e_6)_\parallel$	60	60
K	$\langle\langle B\rangle\rangle^w \cup$ $\{[\langle 0, e_2+e_3, e_2+e_4, e_3+e_4\rangle_\perp \cup$ $\langle e_2+e_3, e_3+e_4, -e_1+e_3,$ $-e_1+e_2+e_3+e_4\rangle_\perp \cup$ $\langle 0, -e_1+e_3, e_2+e_3, e_3+e_4\rangle_\perp]$ $+(e_1-e_6)_\perp\}$	$\{[P(\bar{1}11100)\circ e_3]_\parallel \cup$ $[P(\bar{1}11100)\circ(-e_1+e_2+e_4)]_\parallel\}$ $+(e_1-e_6)_\parallel$	30	30

2.4. Vertex configurations of the tiling $\mathcal{T}^{(D)}$, construction of $\mathcal{T}^{(D)}$

We rederive all representative vertex configurations of Danzer's octahedra using the tools of the projection method (vertex windows and windows for Danzer's octahedra). The results are in agreement with those obtained by Danzer [1] and Kasner [12] through inflation. For each type of vertex configuration (table 5) we list the number of tiles attached to it, the symmetry of the configuration and its relative probability. The three globally icosahedrally-symmetric Danzer tilings (from one point), that produce starting the inflation from icosahedrally-symmetric vertices $7a$, $5b$ and $9c$, can be locally derived from the three corresponding globally icosahedrally-symmetric tilings of $\mathcal{T}^{(2F)}$ such that their projection starts with icosahedrally-symmetric vertices of type a, b and c, respectively [9].

If one wishes to construct the tiling $\mathcal{T}^{(D)}$ by projection, the procedure given in the introduction for the case of generalized windows should be applied. The frequencies of the tiles of $\mathcal{T}^{(D)}$ determined by projection and inflation are clearly in agreement.

3. Conclusion

We have shown that Danzer tiling $\mathcal{T}^{(D)}$ can be locally derived from the tiling $\mathcal{T}^{(2F)}$ of Kramer *et al.* Moreover, we have established the tools needed to obtain $\mathcal{T}^{(D)}$ by projection from the 6D lattice D_6. Meanwhile, Roth [13] and Danzer *et al* [14] have independently shown the equivalence of Danzer tiling with the tiling of Steinhardt and Socolar [15]. Consequently, from the present paper it becomes evident that Steinhardt–Socolar tiling can also be obtained from the D_6 lattice by projection.

The inverse procedure, local derivation of the tiling $\mathcal{T}^{(2F)}$ from the tiling $\mathcal{T}^{(D)}$, is not possible.

Table 5. Vertex configurations of Danzer octahedra tiling determined by projection. Octahedra $\langle\langle X\rangle\rangle$, $X = A, B, C, K$ are additionally described by their vertices. The index by some vertices accounts for the different space angles (see figure 1). For convenience, the relative frequencies are normed to $93 + 149\tau$.

Vertex	$\langle\langle A\rangle\rangle$				$\langle\langle B\rangle\rangle$				$\langle\langle C\rangle\rangle$				$\langle\langle K\rangle\rangle$			Sym.	Relative
number	a	b	c_1	c_2	a	b_1	b_2	c	a_1	a_2	b	c	a	b	c	orient.	frequency
$a.1$					6					1			5			$C_{2v} : 30$	$5 + 20\tau$
$a.2$	3				6				3				3			$C_{3v} : 20$	10
$a.3$					3					3			5			$m : 60$	10
$a.4$										5			5			$C_{5v} : 12$	$-2 + 4\tau$
$a.5$	6				2				11				1			$C_{2v} : 30$	$-15 + 10\tau$
$a.6$	5								20							$C_{5v} : 12$	$14 - 8\tau$
$a.7$									30							$I_h : 1$	$-4 + 3\tau$
$b.1$							1							1		$C_{2v} : 30$	$45 + 70\tau$
$b.2$											3			3		$C_{3v} : 20$	$10 + 20\tau$
$b.3$		4				1					6			1		$C_{2v} : 30$	5
$b.4$		5				10					5					$C_{5v} : 12$	$-2 + 4\tau$
$b.5$						30										$I_h : 1$	$2 + \tau$
$c.1$			1									4			1	$C_{2v} : 30$	$5 + 10\tau$
$c.2$								5				5			5	$C_{5v} : 12$	$6 + 8\tau$
$c.3$				1				16							11	$C_{2v} : 30$	$25 - 10\tau$
$c.4$								15							15	$C_{3v} : 20$	$-30 + 20\tau$
$c.5$				3				13							8	$m : 60$	$-30 + 20\tau$
$c.6$				5				10							5	$C_{5v} : 12$	$14 - 8\tau$
$c.7$								10							20	$C_{2v} : 30$	$65 - 40\tau$
$c.8$								5							25	$C_{5v} : 12$	$-58 + 36\tau$
$c.9$															30	$I_h : 1$	$18 - 11\tau$

Acknowledgments

This work was supported in part by the Deutsche Forschungsgemeinschaft. PK, ZP and MS would like to acknowledge the hospitality of the Zentrum für Interdisziplinäre Forschung, U Bielefeld, Germany, where part of this work was developed during a workshop on the 'Geometry of Quasicrystals' in March, 1991.

References

[1] Danzer L 1989 *Discrete Math.* **76** 1–7

[2] Danzer L 1991 *Quasiperiodicity, Local and Global Aspects (Lecture Notes in Physics 382)* ed V V Dodonov *et al* (Berlin: Springer) 561–72

[3] Baake M, Schlottmann M and Jarvis P D 1991 *J. Phys. A: Math. Gen.* **24** 4637–54

[4] Guryan C A, Goldman A I, Stephens P W, Hiraga K, Tsai A P, Inoue A and Masumoto T 1989 *Phys. Rev. Lett.* **62** 2409–12

[5] Conway J H and Sloane N J A 1988 *Sphere Packings, Lattices and Groups* (New York: Springer)

[6] Kramer P, Papadopolos Z and Zeidler D 1992 The root lattice D_6 and icosahedral quasicrystals *Group Theory in Physics (AIP Conf. Proc. 266)* (New York: AIP) 179–200

[7] Kramer P and Schlottmann M 1989 *J. Phys. A: Math. Gen.* **22** L1097–102

[8] Schlottmann M 1993 *Int. J. Mod. Phys.* B **7** 1351–63

[9] Zeidler D 1992 *PhD Thesis* Tübingen

[10] van Ophuysen 1991 private communication

[11] Papadopolos Z, Kramer P and Zeidler D 1993 *Non-Cryst. Solids* **153&154** 215–20

[12] Kasner G and Böttger H 1993 *Int. J. Mod. Phys.* B **7** 1487–504
[13] Roth J 1993 *J. Phys. A: Math. Gen.* **26** 1455–61
[14] Danzer L, Papadopolos Z and Talis A 1993 *Int. J. Mod. Phys.* B **7** 1379–86
[15] Socolar J E S and Steinhardt P J 1986 *Phys. Rev.* B **34** 617–47